Identification of connectivity in neural networks

Xiaowei Yang* and Shihab A. Shamma*‡§
*Systems Research Center and ‡Electrical Engineering Department and the §University of Maryland Institute for Advanced Computer Studies, University of Maryland, College Park, Maryland 20742 USA

ABSTRACT Analytical and experimental methods are provided for estimating synaptic connectivities from simultaneous recordings of multiple neurons. The results are based on detailed, yet flexible neuron models in which spike trains are modeled as general doubly stochastic point processes. The expressions derived can be used with nonstationary or stationary records, and can be readily extended from pairwise to multineuron estimates. Furthermore, we show analytically how the estimates are improved as more neurons are sampled, and derive the appropriate normalizations to eliminate stimulus-related correlations. Finally, we illustrate the use and interpretation of the analytical expressions on simulated spike trains and neural networks, and give explicit confidence measures on the estimates.

1. INTRODUCTION

Most functions of the mammalian nervous system are performed by networks of highly interconnected neurons. In the experimental study of these networks, extracellular recordings are often employed to sample the patterns of action potentials simultaneously generated by several neurons (2, 9, 15, 16, 19). The correlations among the recorded firings of the different cells are then used as measures of the type and strength of their interconnections. Many such measures have been proposed to accomplish the latter task; they include the cross-interval histograms, the cross-correlation histograms, the cross-covariance histogram, and the joint peri stimulus time (PST) histogram (the scatter diagram) (8, 9). In all cases, the histograms provide statistical measures in support of various hypotheses such as whether the two (or more) neurons under study directly influence each other or simply share common inputs, and whether the influences are excitatory or inhibitory.

There are three basic difficulties with these methods that we tackle in this report. The first concerns the lack of flexible general analytical treatments that outline the relations between the synaptic connectivities and the correlation measures that are used to estimate them. Thus, while various features in the above mentioned histograms may reflect qualitatively the underlying connections, several parameters and conditions can render these measures inadequate. Examples of such difficulties are the differing integrating dynamics of different cell types, and the potentially severe errors due to stimulus-induced (rather than synaptic) correlations. Attempts to overcome these problems, as in the use of the *shuffling method* to reduce stimulus effects, are shown here to be largely inadequate.

The second basic shortcoming of the above correlation methods stems from the nonstationarity of the neural records. In constructing cross-interval and cross-correlation histograms, counts are usually obtained not only by averaging over different stimulus presentation but also by averaging over the time duration of each presentation period. This makes these two estimates inadequate when working with nonstationary records and, instead, measures based on time-dependent histograms such as the joint PST scatter diagram should be used for the analysis (10, 18).

Finally, it is unclear in many existing methods how to extend the analysis to more than two neurons, and how to evaluate the degree to which a pairwise estimate is improved when the records from many other neurons are included. This is a particularly important criterion as progress in multiunit recording technologies which promises to increase significantly the number of records of simultaneously active neurons.

To summarize, the objectives of this paper are (*a*) to provide rigorous analytical and experimental methods to estimate synaptic connectivities from simultaneous recordings of multiple neurons that are based on accurate and flexible neuron models, (*b*) to express synaptic connectivity in terms of probability densities of joint neuronal firings and individual neuronal firings that can be used with nonstationary (or stationary) records, (*c*) to extend these methods from pairwise to multiunit correlations.

The paper is organized as follows. In the next section, a stochastic nonlinear neuron model is proposed, and the spike train generated by the model is expressed by a doubly stochastic process. This model will serve as the fundamental tool upon which the analytical results are

based. In section 3, quantitative analyses of neuronal connectivities are carried out through the model. These include derivations of the relations between the synaptic connectivity and the firing probability densities, and extending the pairwise correlations to the multineuron case. In section 4, the results are summarized and discussed in the context of practical implementations and considerations of the accuracy of the estimates. All the analytical treatments are contained within sections 2 and 3. For the reader interested only in using the final expressions, section 4 outlines the results and is sufficient as a guide for their experimental applications. Finally, the analytical results are simulated and discussed in section 5. The proofs of lemmas and theorems are given in the Appendix.

2. NEURON MODEL

The basic unit of the nervous system which receives and transmits neural signals is the neuron. The interactions of neurons in a network occur in most cases through synaptic connections between them. Most synapses are found between the axon terminals of a presynaptic neuron and the soma of dendritic tree of a postsynaptic neuron. Since there can be many synapses between any two neurons, it is impractical in modeling the neural network to account for individual synapses; rather, it is more fruitful both for experimental investigation and mathematical description to consider the *total effective influence* of one cell on another.

Consider that neuron A is influenced by a family of neurons B_i, $i = 1, 2, \ldots, n$. The model we use is depicted in Fig. 1; it is similar in many respects to that studied by Knox (11) and by van den Boogaard et al. (4). A sequence of impulses from neuron B_i is transformed into a membrane potential in neuron A. The membrane potential W_t^A of neuron A is represented by a linear spatial-temporal superposition of all input action potentials of neurons B_1, B_2, ..., B_n (including self inhibition and/or self excitation), and an unknown random potential U_t which represents the influence of all other unobservable neurons and biophysical factors. A sigmoid function g is used to map the somatic potential as follows:

$$W_t^A = g\left[U_t + \sum_{i=1}^{n} \int_0^t h_i(t, \tau)\, dN_{B_i}(\tau)\right] = g\left[U_t + \sum_{i=1}^{n} \sum_{k=1}^{N_{Bi}(t)} h_i(t, T_k^{B_i})\right], \quad (1)$$

where $\{T_k^{B_i}: k = 1, 2, \ldots\}$ are the epoch times of spike train from neurons B_i, and $\{N_{B_i}(t): t \geq 0\}$ is the associated counting process, i.e., the number of spikes arriving from neuron B_i in the interval $(0, t]$.

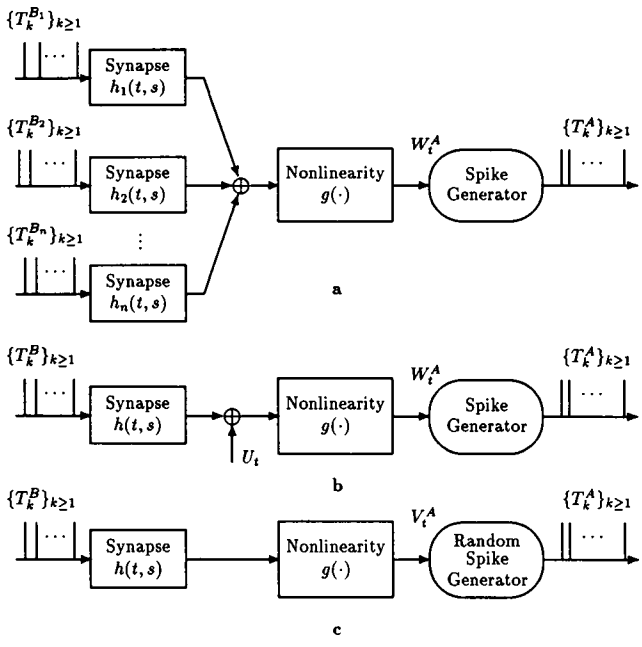

FIGURE 1 A dynamical nonlinear neuron model, where neuron A is considered as the postsynaptic neuron. (*a*) Neuron A is influenced by presynaptic neurons B_1, B_2, ..., B_n. (*b*) A synaptic connection between neurons A and B; the influences of other neurons on neuron A are summarized by U_t. (*c*) An equivalent probabilistic version of the neuron model. The impact of the random input U_t is now moved to the spike generator where the threshold becomes random.

A spike is generated when the integrated membrane potential, $\int_{t_0}^{t} W_\tau^A\, d\tau$, exceeds a stochastic threshold $\theta_w(t)$. The membrane potential then discharges to a resting level v_o, and hence the input information before the firing instant is completely discarded. Denote by $h_i(t, s)$ the impulse response (not necessarily time-invariant) which describes the total temporal influence of neuron B_i on neuron A from past up to present, including the conduction and transmission delay. A synaptic connection is said to be excitatory if $h(t, s) \geq 0$ for all t, all s in the real line R; it is said to be inhibitory if $h(t, s) \leq 0$ for all t, all s in R.

For mathematical simplicity, let us assume that the nonlinearity g has the form of $g(x) = \alpha e^x$, $\alpha > 0$, i.e., that neuron A is operating around threshold and is thus not strongly driven. This form of nonlinearity leads to a multiplicative model, which was used earlier by van den Boogaard (5, 10). Suppose further, without loss of generality, that we are interested in finding the connectivity between two neurons A and B_1. In the following discussion, we write $B = B_1$ and $h(t, s) = h_1(t, s)$ for simplicity. Then,

$$W_t^A = \frac{1}{\alpha} g\left[U_t + \sum_{i=2}^{n} \sum_{k=1}^{N_{Bi}(t)} h_i(t, T_k^{B_i})\right] V_t^A, \quad (2)$$

where V_t^A is called here the *semi-membrane potential* due to neuron B and is defined as

$$V_t^A = g\left[\sum_{k=1}^{N_B(t)} h(t, T_k^B)\right]. \tag{3}$$

To account for the firings of neuron A that are due to V_t^A, we can think of the factor $Z_w(t) = \alpha/g(U_t + \Sigma_{i=2}^{n}\Sigma_{k=1}^{N_{B_i}(t)} \cdot h_i(t, T_k^{B_i}))$ as a positive stochastic process with slow time variation relative to interspike intervals. The slow variation assumption is valid for a neuron influenced by a large pool of neurons where the contribution of each neuron is small. Therefore,

$$\int_{t_0}^{t} W_\tau^A \, d\tau = \int_{t_0}^{t} [V_\tau^A / Z_w(\tau)] \, d\tau \simeq \left[\int_{t_0}^{t} V_\tau^A \, d\tau\right] \Big/ Z_w(t).$$

Then we define an effective threshold $\theta(t) = Z_w(t)\theta_w(t)$. A spike occurs whenever the threshold $\theta(t)$ is exceeded by the accumulated semimembrane potential, i.e.,

$$\int_{t_0}^{t} V_\tau^A \, d\tau > \theta(t), \tag{4}$$

where t_0 is the instant of the preceding spike. In fact, Eq. 4 is equivalent to $\int_{t_0}^{t} W_\tau^A \, d\tau > \theta_w(t)$, described previously. Let Z and $\theta_o(t)$, respectively, absorb all the randomness and all the time variation of both $Z_w(t)$ and $\theta_w(t)$ so that the threshold $\theta(t)$ is comprised of a random variable Z and a time function $\theta_o(t)$ as

$$\theta(t) = Z\theta_o(t). \tag{5}$$

Due to the refractory period r during which a neuron is unable to produce a successive spike, the time function can be taken as simple as

$$\theta_o(t) = \begin{cases} \infty, & T_k \le t < T_k + r \\ \theta_o, & T_k + r \le t < T_{k+1}, \end{cases} \tag{6}$$

where $\theta_o > 0$ is a constant, and T_k and T_{k+1} are the times at which the kth and $(k+1)$-st spike occur, respectively.

Denoting by $N_A(t)$ the number of spikes in train A during time interval $(0, t]$, a stochastic counting process $\{N_A(t): t \ge 0\}$ is associated with spike train A with $N_A(0) = 0$. Let $\Delta N_A(t) = N_A(t + \Delta t) - N_A(t)$ be the number of spikes in an infinitesimal duration Δt. We say that a process is *orderly* if $P_r(\Delta N_A(T) > 1) = o(\Delta t)$. Armed with these general neuron models, we are ready for the analysis of the interneuronal connectivities deduced from the stochastic firing of several neurons.

3. ANALYTICAL RESULTS

In this section, we shall derive and elaborate on three basic results. We shall first consider the simple case of two observable neurons, and show how the connectivity between them can be expressed analytically in terms of the neuron model outlined above. We then consider the sources of uncertainty in this estimate and how they can be reduced through added information from neighboring neurons. Finally, we shall comment on the critical normalization procedures used to remove the confounding effects of stimulus artifacts.

In the following discussion, we will make use of the PST histogram of a single cell spike train which measures the firing rate of a neuron with respect to the stimulus onset. Each bin of the PST histogram is an unbiased estimator for the probability density of the average neuron firing over a short period Δt at instant t corresponding to that bin. Let us denote by $P_A(t)$ the conditional firing probability density of the *postsynaptic* neuron given the history of the intensity process of the presynaptic neuron, $\mathcal{H}_t^B = \sigma\{V_s^B: s \le t\}$, and the history $\mathcal{N}_t^A = \sigma\{N_A(s): s \le t\}$ of spike train A, that is,

$$P_A(t) = \lim_{\Delta t \to 0} \frac{P_r(\Delta N_A(t) = 1 | \mathcal{H}_t^B, \mathcal{N}_t^A)}{\Delta t}. \tag{7}$$

The firing probability density of neuron A is defined as

$$P_r(A_t) = E[P_A(t)] = \lim_{\Delta t \to 0} \frac{P_r[\Delta N_A(t) = 1]}{\Delta t}, \tag{8}$$

where the second equality is obtained by interchanging the limitation and the expectation operations. Because the firing rate of a neuron is finite, this interchangeability is guaranteed by the dominated convergence theorem. This argument applies to every similar situation throughout the paper.

Likewise, denote by $P_B(s)$ is the conditional firing probability density of the *presynaptic* neuron given the history of the intensity process of the presynaptic neuron and the history of spike train B, that is,

$$P_B(s) = \lim_{\Delta s \to 0} \frac{P_r(\Delta N_B(s) = 1 | \mathcal{H}_s^B, \mathcal{N}_s^B)}{\Delta s}. \tag{9}$$

We have

$$P_r(B_s) = E[P_B(s)] = \lim_{\Delta t \to 0} \frac{P_r(\Delta N_B(s) = 1)}{\Delta s}. \tag{10}$$

Note that the individual PST histograms of neurons A and B estimate $E[P_A(t)]\Delta t$ and $E[P_B(s)]\Delta s$, respectively, and that $P_B(s)$ is *not* defined symmetrically to $P_A(t)$.

Moreover, the joint PST histogram of the two neurons estimates $E[P_{AB}(t, s)]\Delta t \Delta s$, where $P_{AB}(t, s)$ represents the conditional joint probability density of firing of neurons A and B,

$$P_{AB}(t, s) = \lim_{\Delta t, \Delta s \to 0} \frac{P_r(\Delta N_A(t) = 1, \Delta N_B(s) = 1 | \mathcal{H}_{\max(t,s)}^B, \mathcal{N}_t^A, \mathcal{N}_s^B)}{\Delta t \Delta s} \tag{11}$$

and

$$P_r(A_t, B_s) = E[P_{AB}(t,s)] = \lim_{\Delta t, \Delta s \to 0} \frac{P_r[\Delta N_A(t) = 1, \Delta N_B(s) = 1]}{\Delta t \Delta s}. \quad (12)$$

Recall that $h(t,s)$ represents the synaptic connectivity between neurons A and B. The three basic results derived are as follows.

Result 1

The joint probability density of firing of a presynaptic and postsynaptic neuron pair can be expressed as the product of individual firing probability densities and the pairwise connectivity, and a corrupting (uncertainty) factor due to other unobservable influences on the firing of A:

$$P_r(A_t, B_s) = P_r(A_t) P_r(B_s) \gamma(t, s) e^{h(t,s)}, \quad (13)$$

where $\gamma(t, s)$ is the corrupting factor ($\gamma \geq 0$) given by

$$\gamma(t, s) = \frac{E[f_A(t, \theta_t^A) P_B(s)]}{E[f_A(t, \theta_t^A)] E[P_B(s)]}, \quad (14)$$

where

$$f_A(t, \theta_t^A) = V_t^A \frac{f_{\theta_t^A}(a_t)}{1 - F_{\theta_t^A}(a_t)}, \quad (15)$$

where $a_t = \int_{t_0}^{t} V_\tau^A \, d\tau$, and $f_{\theta_t^A}(\cdot)$, $F_{\theta_t^A}(\cdot)$ are the density and the distribution functions of the threshold of neuron A, respectively.

Result 2

The uncertainty can be reduced (i.e., the corrupting factor can be made closer to 1) if more interacting neurons $C_1, C_2, \ldots, C_m$ are observed simultaneously. If $P_r(A_t, C_t) \neq 0$ and $P_r(B_s, C_t) \neq 0$, then the pairwise connectivity becomes

$$h(t, s) = \log \frac{P_r(A_t, B_s, C_t) P_r(C_t)}{P_r(A_t, C_t) P_r(B_s, C_t)} - \log \gamma^*, \quad (16)$$

with $C_t = \{\bigcap_i^m {}_{-1} C_i \text{ fires in } (t, t + \Delta t)\}$, where

$$\gamma^*(t, s) = \frac{E[f_A(t, \theta_t^A) P_B(s) | C_t]}{E[f_A(t, \theta_t^A) | C_t] E[P_B(s) | C_t]} \quad (17)$$

is a quantity satisfying $|\gamma^* - 1| \leq |\gamma - 1|$. If γ^* is very close to 1, then $\log \gamma^*$ can be neglected.

Result 3

To minimize the effects of the stimulus on the estimators of the connectivity, the normalized joint probability of firing given by

$$N_p(t, s) = P_r(A_t, B_s) / P_r(A_t) P_r(B_s) \quad (18)$$

leads to estimators superior to those produced by the often employed *shuffle* method (normalization by difference):

$$N_d(t, s) = P_r(A_t, B_s) - P_r(A_t) P_r(B_s), \quad (19)$$

which is the quantity that the cross-covariance histogram estimates.

3.1 Further relationships

To discuss the derivation of the above stated results, we will need to utilize a few more relationships. Given a pair of interacting neurons (A and B), the following lemmas will play an important role in the analysis below. Let us first define an auxillary function:

$$f_B(t, \theta_t^B) = \lim_{\Delta t \to 0} \frac{P_r(\Delta N_B(t) = 1 | \theta_t^B; \mathcal{H}_t^B, \mathcal{N}_t^B)}{\Delta t}. \quad (20)$$

Lemma 1. $P_B(t)$ can be expressed as a map from the semi-membrane potential space of neuron B onto $[0, \infty)$,

$$P_B(t) = V_t^B E_{b_t}[f_B(t, \theta_t^B)] \quad (21)$$

with

$$f_B(t, \theta_t^B) = V_t^B \frac{f_{\theta_t^B}(b_t)}{1 - F_{\theta_t^B}(b_t)}, \quad (22)$$

where $b_t = \int_{t_0}^{t} V_\tau^B \, d\tau$, and $f_{\theta_t^B}(\cdot)$, $F_{\theta_t^B}(\cdot)$ are the density and the distribution functions of the threshold of neuron B, respectively. The expectation $E_{b_t}[\cdot]$ is taken with respect to θ_t^B. The function $P_B(\cdot)$ can have a very simple form. For example, if the threshold is an exponentially distributed independent random variable with mean λ, then $P_B(t) = \lambda V_t^B$. And in this case, $\{N_B(t): t \geq 0\}$ is a doubly stochastic Poisson process.

Lemma 2. The conditional expectation of the product of the semi-membrane potential of neuron A and the firing rate of neuron B can be expressed as

$$E\left[V_t^A \frac{dN_B(s)}{ds}\right] = e^{h(t,s)} E[V_t^A P_B(s)]. \quad (23)$$

3.2 Discussion of result 1

We will first need to derive an expression for the firing rate of the postsynaptic neuron (A). In general, the threshold θ_t^A of this neuron is not an independent variable, because it depends on all other unobservable inputs to the neuron. Given an arbitrary value for θ_t^A, we define

$$f_A(t, \theta_t^A) = \lim_{\Delta t \to 0} \frac{P_r(\Delta N_A(t) = 1 | \theta_t^A; \mathcal{H}_t^A, \mathcal{N}_t^A)}{\Delta t}. \quad (24)$$

Note that $f_A(t, \theta_t^A)$ is a symmetry to $f_B(t, \theta_t^B)$ defined in Eq. 20, and is *not* $P_A(t)$ defined in Eq. 7. By lemma 1 we

have

$$P_r(A_t) = E[f_A(t, \theta_t^A)] = E\left[V_t^A \frac{f_{\theta_t^A}(a_t)}{1 - F_{\theta_t^A}(a_t)}\right], \quad (25)$$

where $a_t = \int_{t_0}^{t} V_\tau^A \, d\tau$, and $f_{\theta_t^A}(\cdot)$, $F_{\theta_t^A}(\cdot)$ are the density and the distribution functions of the threshold of neuron A, respectively.

Similarly, the joint probability density of firing can be expressed as

$$P_r(A_t, B_s) = e^{h(t,s)} E[f_A(t, \theta_t^A) P_B(s)]. \quad (26)$$

Because the firing probability density of the presynaptic neuron is

$$P_r(B_s) = E[P_B(s)], \quad (27)$$

then combining Eqs. 26, 25, and 27 gives result 1 with

$$\gamma(t, s) = \frac{E[f_A(t, \theta_t^A) P_B(s)]}{E[f_A(t, \theta_t^A)] E[P_B(s)]}. \quad (28)$$

3.3 Discussion of result 2

The factor $\gamma(t, s)$ reflects our ignorance of the input to neuron B, or that of the knowledge of the effective threshold θ_t^A. There are conceptually two ways in which the uncertainty can be reduced (i.e., $\gamma(t, s) \to 1$):

(a) For a completely known input $\{V_s^B\}$ (hence $P_B(s)$ is determined), $\gamma(t, s) = 1$. This can be achieved experimentally if each realization of spike train B is identical. For instance, one may produce deterministic spike pattern in neuron B using electrical stimulation. Alternatively, one may construct a *cross-interval histogram* (8) (also called a *cross-renewal histogram* [1]) using each spike in neuron B as a reference time to estimate $P_r(A_{t-s}, B_s)$ (and hence $h[t - s]$). This is of course only valid if $h(t)$ is time invariant and short relative to the interspike intervals of neuron B (i.e., the histogram trials are independent). One can avoid dependent histogram trials by constructing instead a conditional histogram given previous spikes in neuron B which estimates $P_r(A_{t-s}, B_s \mid \text{previous } B \text{ spikes at } s_1, s_2, \ldots, s_k)$, where dependence is assumed to be limited to at most k consecutive spikes in neuron B. The connectivity is then given by $h(t - s) = \ln [P_r(A_{t-s}, B_s \mid \text{previous } B \text{ spikes at } s_1, s_2, \ldots, s_k) / P_r(A_{t-s} \mid \text{previous } B \text{ spikes at } s_1, s_2, \ldots, s_k)]$.

(b) The alternative way is to make $f_A(t, \theta_t^A)$ more deterministic (decreasing the variance). This occurs if we know more about θ_t^A (comprising the intrinsic threshold $\theta_w[t]$ and the unknown source $Z_w[t]$). Intracellular measurements of neuron A obviate the need for $\theta_w(t)$ and give complete information regarding $Z_w(t)$. However, where only extracellular recording are possible, information about $Z_w(t)$ may be obtained from measurements of more neurons. For instance, if the activities of more interacting neurons $(C_1, C_2, \ldots, C_m)$ are available, we can use a multiunit PST histogram in addition to the conventional joint and individual histograms to estimate

$$\frac{P_r(A_t, B_s, C_t) P_r(C_t)}{P_r(A_t, C_t) P_r(B_s, C_t)} = \frac{P_r(A_t, B_s \mid C_t)}{P_r(A_t \mid C_t) P_r(B_s \mid C_t)} = \gamma^*(t, s) e^{h(t,s)}, \quad (29)$$

where $\gamma^*(t, s)$ is defined in Eq. 17.

Because neurons $(C_1, C_2, \ldots, C_m)$ may contain information about $P_B(s)$ and/or θ_t^A (for instance, if these neurons influence the activity of either or both neurons A and B), observing more interacting neurons makes $f_A(t, \theta_t^A)$ less correlated with $P_B(s)$. Consequently, observing more neurons makes γ^* closer to one than γ is in Eq. 28, and hence the estimator for $h(t, s)$ is more reliable.

The estimates computed from results 1 and 2 are superior to those obtained from the cross-correlation function which, as Knox pointed out in reference 11, yields *biased* estimates of the postsynaptic potential (PSP) shape (i.e., the $h[t, s]$), and the amount of bias can only be determined empirically. Instead, in our estimates, the connectivity can be estimated by the normalized joint PST histogram along with an uncertainty factor, and this uncertainty can be explicitly expressed under appropriate conditions (see following theorem 2). Furthermore, it is possible to reduce it by increasing the number of observed neurons.

3.4 Special case discussion

To illustrate this with explicit analytic expressions, three simplifying assumptions will be adopted concerning the properties of the postsynaptic neuron threshold θ_t^A (used in theorem 1 below) and the distribution of the presynaptic potential (used in theorem 2). We start by stating two of these assumptions and the theorems associated with them, and then proceed to relate the correlation functions explicitly to the interneuronal connectivity ($h[t, s]$) in a pair of neurons (A and B).

Assumption 1. The random variable Z of the threshold in Eq. 5 is independent of V_t^A, and has an exponential pdf:

$$p_z(z) = \begin{cases} \theta_o e^{-(\theta_o z - v_o)}, & v_0/\theta_o \le z < \infty \\ 0, & z < v_o/\theta_o, \end{cases} \quad (30)$$

where $\theta_o > 0$, and v_o is a resting level of the membrane potential.

This assumption is typically valid in cases where neuron A is only related to neuron B, i.e., it is weakly related to any other neuron. It can be verified that under assumption 1, the output spike train of the neuron A is a doubly stochastic Poisson process $\{N_A(t): t \ge 0\}$ with the intensity

process $\{\Lambda_t^A: t \geq 0\}$, where

$$\Lambda_t^A = \begin{cases} 0, & T_k \leq t < T_k + r \\ V_t^A, & T_k + r \leq t < T_{k+1}, \end{cases} \tag{31}$$

where r is the refractory period. Note that Λ_t^Adepends on $\mathcal{N}_t^A$, and hence $\{N_A(t): t \geq 0\}$ is a self-exciting process with the intensity function $E[\Lambda_t^A|\mathcal{N}_t^A]$ (17).

Assumption 2. The refractory period is much smaller than any interspike interval and hence is negligible.

Under this assumption Λ_t^A does not depend on $\mathcal{N}_t^A$, and hence the intensity process becomes the membrane potential process. The following theorem is a typical result of the multiplicative model first found by Brillinger (6), and we restate it here in a more general fashion.

Theorem 1

(*a*) Under assumptions 1 and 2, $\{N_A(t): t \geq 0\}$ is a doubly stochastic Poisson process with the intensity process $\{V_t^A: t \geq 0\}$. (*b*) In this case, the conditional joint probability density of firing of neurons A and B can be expressed as

$$P_{AB}(t, s) = P_A(t)P_B(s)e^{h(t,s)} \tag{32}$$

for all t and all s, where $h(t, s)$ is the interneuronal connectivity with nonzero transmission delay.

Theorem 1 states that the conditional joint probability density of firing can be expressed as the product of the conditional individual firing densities and the connectivity. Thus the interneuronal connectivity $h(t, s)$ could be directly identified by

$$h(t, s) = \log P_{AB}(t, s) - \log P_A(t) - \log P_B(s). \tag{33}$$

Assertion *b* in the above theorem includes the special case where the input process is Poisson, which was previously obtained by van de Boogaard et al. from the expansion approach of the characteristic functional of the input and the output processes (4).

However, because the membrane potentials are unobservable in extracellular recordings, the semimembrane potential of the presynaptic neuron B is generally unknown (hence P_A, P_B, and P_{AB} are unknown). Therefore, one must instead evaluate the normalized *unconditional* joint probability density:

$$N_p(t, s) = \frac{E[P_{AB}(t, s)}{E[P_A(t)]E[P_B(s)]}, \tag{34}$$

which is the cross-product ratio described in reference 6. The connectivity $h(t, s)$ can not be accurately estimated in general.

Assumption 3. The semimembrane potential process of the presynaptic neuron can be decomposed in the form of $V_t^B = Xf(t)$, where X is gamma distributed with parameters (λ, υ), and $f(t)$ is a deterministic time function.

Theorem 2

If assumptions 1, 2, and 3 hold, the uncertainty γ in result 1 can be expressed as

$$\gamma(t, s) = \frac{\lambda}{\lambda - \eta_t}, \quad \eta_t < \lambda, \tag{35}$$

where

$$\eta_t = \int_0^t (e^{h(t,s)} - 1)f(\tau)\, d\tau. \tag{36}$$

One consequence of theorem 2 is that if assumption 3 holds (a relatively common occurrence [3, 7, 13]), the normalized unconditional joint probability density $N_p(t, s)$ can be explicitly evaluated in terms of these parameters as

$$N_p(t, s) = \frac{\lambda}{\lambda - \eta_t} e^{h(t,s)}, \quad \eta_t > \lambda. \tag{37}$$

Therefore, for a given gamma distribution (of degree υ), as the variance of $X (= \upsilon/\lambda^2)$ becomes smaller, λ increases, and $\gamma(t, s) \rightarrow 1$. In other words, the more is known about V_t^B (e.g., from recordings of additional neurons), the more accurate is the estimate of the connectivity between neurons A and B. We will illustrate these results further through simulations later in section 5 (see Fig. 5).

3.5 Discussion of result 3

An important factor in correctly interpreting the correlations among the activities of different cells concerns the effects of the stimulus. Specifically, this refers to the fact that unconnected cells may exhibit strong correlations in their firings purely due to the fact that they are driven by the same stimulus. To eliminate these effects, some form of normalization is necessary. In result 3 we show how the stimulus shuffle alone fails to accomplish this task. A general discussion of different normalizations can be found in reference 14.

If the membrane potential does not vary much for different stimulus presentation (small variance of X), then $\lambda \gg \eta_t$. Consequently, from Eq. 37 we have

$$N_p(t, s) \simeq e^{h(t,s)}. \tag{38}$$

This confirms the conclusions established in result 2 earlier.

In contrast to the normalization used in Eq. 18, the conventional cross-covariance histogram (which is the modified joint PST diagram using the shuffling method) uses a *difference* normalization which estimates (8, 10):

$$N_d(t, s) = E[P_{AB}(t, s)] - E[P_A(t)]E[P_B(s)]. \tag{39}$$

In general, this expression is very complicated. However, if we make use of assumptions 3, it reduces to

$$N_d(t, s) = \alpha v f(s) M(\eta_t)\left(\frac{e^{h(t,s)}}{\lambda - \eta_t} - \frac{1}{\lambda}\right), \tag{40}$$

where $m(\cdot)$ is the moment generating function of X.

If the membrane potential is not varying too much for different stimulus presentation ($\lambda \gg \eta_t$), then $N_d(t,s)$ can be approximately written as

$$N_d(t, s) \simeq \frac{\alpha v f(s)}{\lambda}(e^{h(t,s)} - 1). \tag{41}$$

This expression suggests that identifying the connectivity here is considerably more difficult than that of the normalization $N_p(t, s)$ used earlier (see Eq. 38), since quantities α, v, λ, and function $f(s)$ are generally unknown. Nevertheless, Eq. 41 suggests that the shuffling method remains effective in indicating *the absence of a direct connection* (i.e., when $h[t, s]$ is very small), because in that case $N_d(t, s)$ is approximately zero regardless of the confounding terms (α, v, λ, and function $f[s]$). We will illustrate this in simulations in section 5 (see Fig. 6).

4. EXPERIMENTAL CONSIDERATIONS

In the analysis of multineuronal connectivities, spike trains from several neurons are recorded in response to the repeated presentation (e.g., R times) of a stimulus. Spikes are usually sampled and parsed into (i.e., labeled by) small time bins in which at most one spike may occur in each bin (which corresponds to the orderliness of the point process). Thus each spike train is converted into a discrete 0–1 process, and is further segmented into R segments, each for one stimulus presentation. Let A_{rn} be the time bin corresponding in the nth bin associated with the rth stimulus presentation. A spike train can then be represented by a $R \times N$ random matrix **A** with elements A_{rn}, ($r = 1, 2, \ldots, R$; $n = 1, 2, \ldots, N$), which is called here a *spike matrix*.

The PST histogram reflects the stimulus-locked firing rate of each single neuron, and it is formed by taking average over every column of the spike matrix,

$$H_n^A = \frac{1}{R}\sum_{r=1}^{R} A_{rn}, \quad n = 1, 2, \ldots, N. \tag{42}$$

The value of H_n^A counts the average spikes over R stimulus presentations in the nth bin in a spike train A. The joint PST scatter diagram of two neurons A and B (H_{mn}^{AB}, $m = 1, 2 \ldots, N$; $n = 1, 2, \ldots, N$) measures the coincidence spikes in train A and in train B relative to stimulus onset. It is a two-dimensional histogram with one axis (m) for train A and the other axis (n) for train B, and hence it is an N square matrix **H**. Element H_{mn}^{AB} represents the average count for coincidence of a spike in the mth bin of train A and a spike in the nth bin of train B over R stimulus presentations, that is,

$$H_{mn}^{AB} = \frac{1}{R}\sum_{r=1}^{R} A_{rm}B_{rn}, \quad m = 1, 2, \ldots, N; \quad n = 1, 2, \ldots, N, \tag{43}$$

where A_{rm} and B_{rn} are the elements of spike matrices for trains A and B, respectively. Therefore, the matrix presentation of the joint PST scatter diagram is

$$\mathbf{H} = \frac{1}{R}\mathbf{A}^T\mathbf{B}, \tag{44}$$

where T denotes transposition. The expanded joint PST histogram for multiunit recordings (of M neurons) is then

$$H_{n_1 n_2 \ldots n_M}^{C_1 C_2 \ldots C_M} = \frac{1}{R}\sum_{r=1}^{R} C_{rn_1}^1 C_{2n_2}^2 \ldots C_{rn_M}^M, \tag{45}$$

where $C_{rn_i}^i$, ($i = 1, 2, \ldots, M$), is the element of the spike matrix for the ith neuron.

4.1 Using the scatter plot to determine neuronal connectivities

The correlations between a pair of recorded neurons (A and B) can be computed from the experimental estimate of the expression of result 1, i.e.,

$$h(t, s) = \log\left(\frac{N_p(t, s)}{\gamma(t, s)}\right)$$

$$= \log\left(\frac{E[P_{AB}(t, s)]}{E[P_A(t)]E[P_B(s)]}\right) - \log[\gamma(t, s)],$$

where $E[P_A(t)]$ and $E[P_B(s)]$ represent the PST histograms of firings of the neuron pair, $E(P_{AB}(t, s)]$ is their scatter plot, and $\gamma(\geq 0)$ is the corrupting factor representing the uncertainty in the estimate due to the influences of other unobserved neurons and biophysical factors. Thus in terms of bin numbers m and n, the above equation can be written as

$$\log\left(\frac{H_{mn}^{AB}}{H_m^A H_n^B}\right) = h(m\Delta t, n\Delta t) + \log[\gamma(m\Delta t, n\Delta t)]. \tag{46}$$

In the case of time invariant connectivities, $h(t, s)$ becomes $h(t - s)$, and the correlation peak becomes a band that runs parallel to the principal diagonal ($t - s = 0$).[1]

[1]Note that one can detect further correlations in the *unnormalized* scatter plot, such as the more diffuse bands of time-invariant common inputs (20). Of course, these features are intentionally removed by the normalization because they do not reflect direct connectivities within the neuron pair.

In the practical application of Eq. 46, the confounding $\gamma(t, s)$ contributions are not known. However, the analysis shows that additional simultaneous recordings can be used to reduce these uncertainties. Therefore, by using the additional data, the improved estimator for $h(t, s)$ becomes

$$\log\left(\frac{H^{ABC_3\ldots C_M}_{mnm\ldots m}\, H^{C_3\ldots C_M}_{m\ldots m}}{H^{AC_3\ldots C_M}_{mm\ldots m}\, H^{BC_3\ldots C_M}_{nm\ldots m}}\right) = h(m\Delta t, n\Delta t) + \log\left[\gamma^*(m\Delta t, n\Delta t)\right], \quad (47)$$

where $H^{C_1C_2\ldots C_M}_{n_1n_2\ldots n_M}$ are simply the joint multidimensional scatter plots defined in Eq. 45, and the uncertainty factor γ^* ($\leq\gamma$) is defined in Eq. 17. The estimates of Eqs. 46 and 47 are illustrated in network simulations in section 5. Other methods to reduce γ are discussed in section 3.3.

4.2 Establishing confidence measures on the estimates

The histograms are random variables subject to fluctuations. Hence, it is important to determine upper and lower bounds such that we assume a connection between neurons A and B whenever these bounds are surpassed. By the law of large numbers, H^{AB}_{mn} converges to $E[P_{AB}(t, s)]$, so does H^{A}_{m} to $E[P_A(t)]$ and H^{B}_{n} to $E[P_B(s)]$ almost surely as $R \to \infty$. Therefore, if neurons A and B are independent, by theorems on limiting distributions,

$$\frac{H^{AB}_{mn}}{H^{A}_{m}H^{B}_{n}} \to 1 \text{ as } R \to \infty \quad (48)$$

almost surely. The hypothesis $\mathcal{H}_0$ is that the two neurons are statistically independent, which is supported by

$$E[P_{AB}(t, s)] = E[P_A(t)]\,E[P_B(s)]. \quad (49)$$

And the alternative hypothesis $\mathcal{H}_1$ is that the two neurons depend, which is described by

$$E[P_{AB}(t, s)] \neq E[P_A(t)]\,E[P_B(s)]. \quad (50)$$

One expects $H^{AB}_{mn}/(H^{A}_{m}H^{B}_{n})$ to be close to 1 if hypothesis $\mathcal{H}_0$ is true. Conversely, if the amount it deviates from 1 exceeds a bound b, one accepts hypothesis $\mathcal{H}_1$. Now for a given significance level α, we need to find the bound b satisfying

$$P_r\left(\left|\frac{H^{AB}_{mn}}{H^{A}_{m}H^{B}_{n}} - 1\right| > b \,\middle|\, H^{A}_{m}, H^{B}_{n}, \mathcal{H}_0\right) = \alpha. \quad (51)$$

The hypothesis testing is stated as the following theorem.

Theorem 3

Let b be a bound which divides a critical region for the hypothesis testing. One announces that there is a depen-

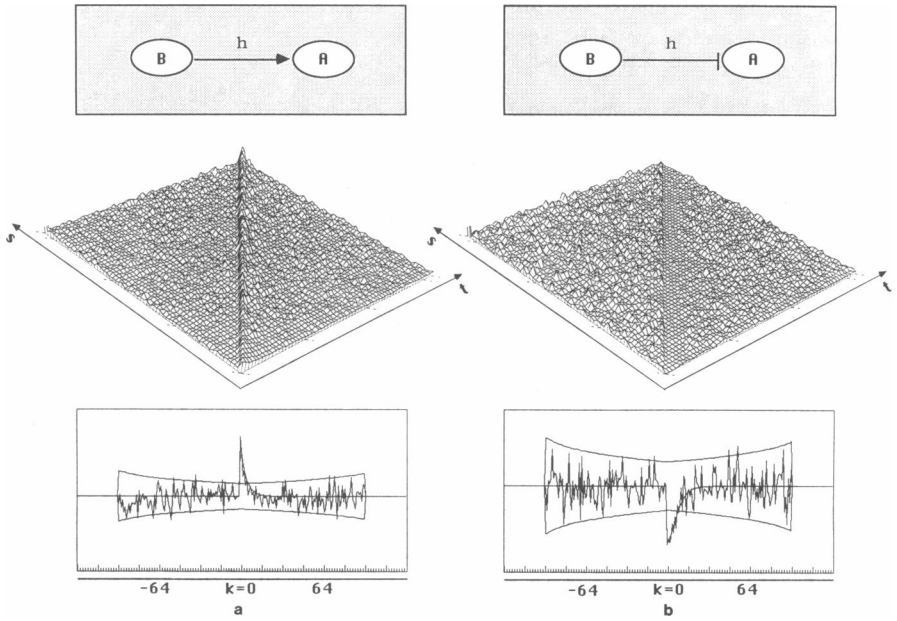

FIGURE 2 Simulations for pairwise excitatory and inhibitory correlations. (*a*) Excitatory coupling $h(t, s) = 0.8e^{-20(t-s)}$, $t > s$. Shown is the two-dimensional normalized scatter plot generated by the spike trains of the two neurons; below it is the histogram G_k that results from collapsing the scatter plot along the principal diagonal. It corresponds to the function $N_p(k) = e^{h(k)}$. The upper and lower bound lines represent the 95% confidence measure. (*b*) Inhibitory coupling, similar to *a* for $h(t, s) = -3.0e^{-20(t-s)}$, $t > s$.

dence between the two observed neurons if

$$\left| \frac{H^{AB}_{mn}}{H^{A}_{m} H^{B}_{n}} - 1 \right| > b. \tag{52}$$

For the given significance level α of false announcement of dependence, the bound can be approximately calculated by

$$b \simeq \epsilon_b \sqrt{\frac{1 - H^{A}_{m} H^{B}_{n}}{R H^{A}_{m} H^{B}_{n}}}, \tag{53}$$

where the value of ϵ_b is determined from

$$\Phi(\epsilon_b) = 1 - \frac{\alpha}{2}, \tag{54}$$

and $\Phi(x) = 1/\sqrt{2\pi} \int_{-\infty}^{x} e^{-x^2/2}\, dx$.

The function $\Phi(x)$ is usually available as the standard normal distribution table. For example, $\alpha = 0.05$ gives $\epsilon_b = 1.96$. The above theorem implies that element $H^{AB}_{mn}/(H^{A}_{m} H^{B}_{n})$ of the normalized joint PST diagram has a conditional expectation value 1 and an approximate conditional variance

$$\sigma^2_{mn} \simeq \frac{1 - H^{A}_{m} H^{B}_{n}}{R H^{A}_{m} H^{B}_{n}}, \tag{55}$$

given the values of H^{A}_{m} and H^{B}_{n} under hypothesis $\mathcal{H}_0$. Because H^{A}_{m} and $H^{B}_{n}$are usually very small and R is fairly large, this approximation is close to a recent result by Palm et al. (14) where their conditional variance is

$$\sigma^2_{mn} = \frac{(1 - H^{A}_{m})(1 - H^{B}_{n})}{(R - 1) H^{A}_{m} H^{B}_{n}} \tag{56}$$

under hypothesis $\mathcal{H}_0$.

The bound dividing the hypothesis regions can be made more useful in neural networks with time-invariant connectivities. Let w_m reflect the fluctuation in the normalized joint PST diagrams such that

$$\frac{H^{AB}_{mn}}{H^{A}_{m} H^{B}_{n}} = \gamma(m\Delta t, n\Delta t) e^{h((m-n)\Delta t)} + w_m, \tag{57}$$

and the mean of w_n is zero. Let $k = m - n$. A collapsed version can be generated by averaging over diagonals of the normalized joint PST diagram. This collapsed version is a one-dimensional histogram G_k expressed by:

$$G_k = \frac{1}{N - |k|} \sum_{n=\max(1,1-k)}^{\min(N,N-k)} \frac{H^{AB}_{n+k,n}}{H^{A}_{n+k} H^{B}_{n}}$$

$$k = -N + 1, \ldots, -1, 0, 1, \ldots, N - 1, \tag{58}$$

where $k = 0$ is the collapsed point of the principal diagonal. Because averaging reduces the fluctuations (the average of w_m has a smaller variance), G_k is a better estimator for the time-invariant connectivity $h(t, s) = h(t - s)$. This enables us to establish a bound such that

$$P_r(|G_k - 1| > b_k | \mathcal{H}_0) = \alpha. \tag{59}$$

Theorem 4

Given a significance level α, let b_k be a bound of critical region satisfying the above equation, then b_k may be approximately written as

$$b_k \simeq \frac{\sqrt{\sum_{n=\max(1,1-k)}^{\min(N,N-k)} \sigma^2_{n+k,n}}}{N - |k|} \epsilon_b, \tag{60}$$

where ϵ_b is the same as in theorem 3, and σ^2_{mn} is given by Eq. 55. Furthermore, b_k will reduce to

$$b_k \simeq \frac{b}{\sqrt{N - |k|}} \tag{61}$$

when σ^2_{mn}'s are taken as constants.

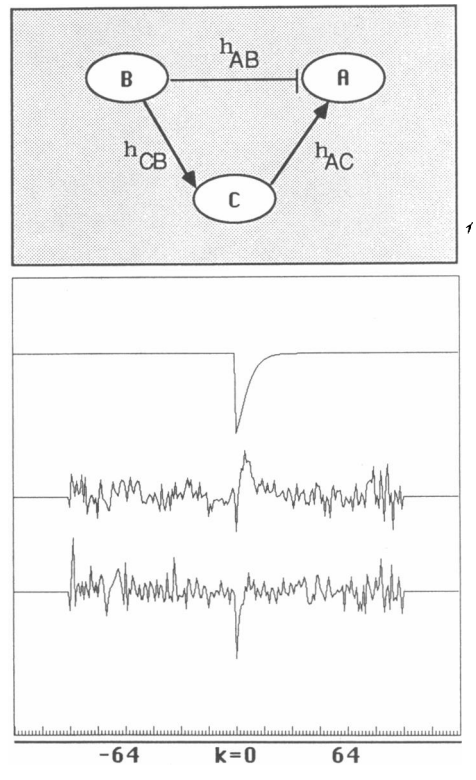

FIGURE 3 Interaction among three neurons. The network structure is displayed on the top graph: neuron B inhibits neuron A and excites neuron C, and neuron C excites neuron A. $h_{AB}(t) = -1.8e^{-20t}$, $h_{AC}(t) = 3.6e^{-20t}$, and $h_{CB}(t) = 2.0e^{-20t}$. The top curve gives the theoretical connectivity from formula 29 with $\gamma^*(t, s)$. The middle one is the correlation curve corresponding to formula 46 generated from spike trains A and B only. The correlation is so distorted that actual inhibition becomes a false excitation (which is actually due to a strong excitatory input from neuron C). The bottom curve shows the tripartite correlation according to formula 47, which displays the correction inhibitory sign for the connectivity.

This theorem indicates that the critical region is enlarged (the bound value decreases) when the collapsed version of the normalized joint PST histogram is used.

5. SIMULATIONS AND DISCUSSION

To illustrate the nature of the estimates, uncertainties, and bounds derived earlier, we show the results from simulations of networks of excitatory and inhibitory neurons. The neuron model used for the simulations is depicted in Fig. 1 *c* where the nonlinearity $g(x) = e^x$ and the random threshold has an exponential distribution with mean 1. The resulting output process of each neuron is a doubly stochastic Poisson process with the intensity process $g[\Sigma_i \Sigma_{k=1}^{N_{B_i}(t)} h_i(t, T_k^{B_i})]$, where the input process $\{T_k^{B_i}: k = 1, 2, \ldots\}$ is the output process of neuron B_i.

In the first case (Fig. 2), for pairwise excitatory and inhibitory, time-invariant connections are estimated using the normalized scatter plots; the uncertainty factor (γ) is equal to 1. The upper plots show the two-dimensional normalized scatter plots. The correlations appear as bands along the principal diagonal because $h(t, s)$ is time-invariant. Hence, the scatter plot can be collapsed along this axis to produce the lower histograms. Note that time variations in $h(t, s)$ (e.g., due to poststimulus adaptation) do not allow this reduction. Consequently, it should only be performed on the portions of the neural record that display obvious stationary behavior. In both simulations of Fig. 2, the predicted analytical estimates are also plotted for comparison, together with the bound lines for the confidence measures (determined by theorem 4).

To illustrate the effects of the uncertainty factor γ, we examine in Fig. 3 the interactions among three neurons with time-invariant connectivities. Here, neuron A is inhibited by neuron B and excited by neuron C, and neuron C is in turn excited by neuron B. Because of the interactions between B and C, the threshold in neuron A is no longer independent of the firings of B. Thus, if we attempt to identify the connectivity between neurons A and B from pairwise recordings, the estimates will be

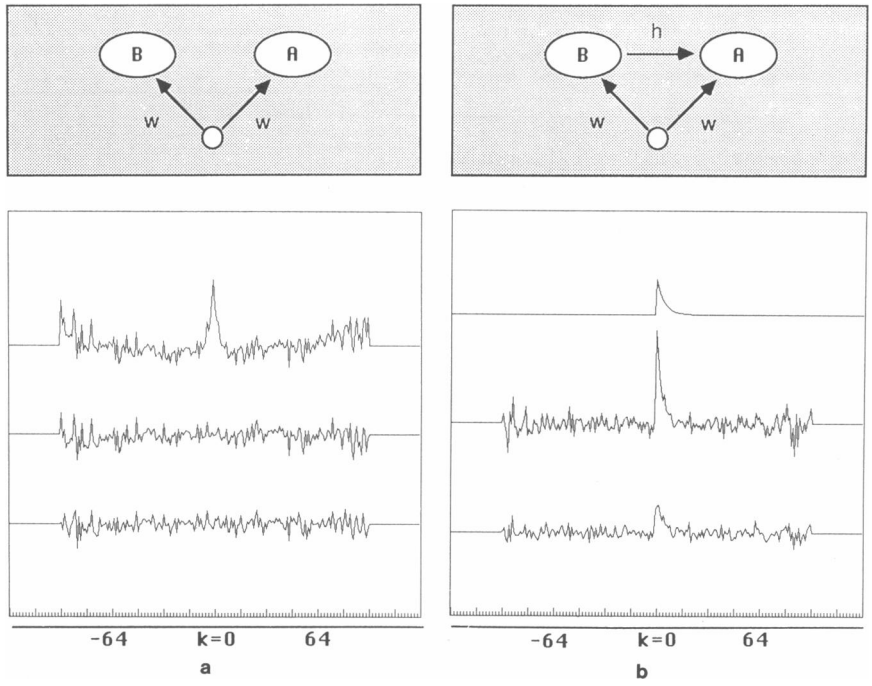

FIGURE 4 Comparison of the preferred normalization with the difference normalization (shuffle method). (*a*) The absence of a direct connection case ($h = 0$). Neurons A and B have a common input source: a neuron driven by a stimulus. The connection strength from the common input is $w = 1$. Top curve gives the collapsed version of the joint PST histogram without any normalization. The correlation peak is purely due to stimulus effects. Middle curve represents the difference normalized correlation. Bottom curve shows the preferred normalized correlation curve. Both methods perform well in indicating the absence of connection between A and B. (*b*) The presence of a direct connection case ($h \neq 0$): Neurons A and B have a common input source as in *a*, and in addition, a direct synaptic connectivity from B to A, $h_{AB}(t) = 0.4e^{-20t}$. Top curve gives the theoretical correlation predicted from $N_p(k) = e^h(k)$. Middle curve shows the difference normalized correlation. Although the connectivity is weak (only 0.4), the large sharp peak in the correlation leads to a false impression of high excitatory connectivity, which is in fact due to stimulus effects. The bottom curve shows the preferred normalized correlation, which is very close to the theoretical function $0.4e^{-20t}$.

contaminated by the γ uncertainty factor. The top curve in Fig. 3 first shows the "target" theoretical connectivity obtained from the multirecording estimate given by formula 29 with $\gamma^*(t, s) = 1$ (i.e., $e^{h_{AB}(t-s)}$). If neuron C is ignored, the pairwise estimate of $e^{h_{AB}(t-s)}$ is shown as the middle curve in Fig. 3 (corresponding to formula 46). The correlation is so distorted that actual inhibition becomes false excitation because of the strong excitatory activity from neuron C. To correct the erroneous correlation, we have to use the information from the third neuron. The tripartite correlation according to formula 47 is displayed at bottom of Fig. 3, which is much closer to the analytical estimate.

Fig. 4 compares the preferred normalization with the difference normalization (shuffle method) under two situations. In the absence of a direct connection, the shuffle method provides accurate indication of the lack of synaptic inputs between the two neurons. However, in the presence of a direct connection, the shuffle method fails to remove completely the stimulus correlations as indicated by the deviation from the analytical results. Instead, the normalization suggested in this paper performs well in both cases.

In conclusion, the above simulations confirm the proposed theory. The neuron model adopted is quite general because (*a*) the synaptic connectivity $h(t, s)$ represents a time-varying system, (*b*) the processes representing spike trains are not necessarily Poisson processes, and (*c*) the nonlinear function $g(x) = \alpha e^x$ is an approximation of $\alpha e^x/1 + \alpha e^x$ when $\alpha e^x \ll 1$, meaning that the neuron is operating at low firing rates. Moreover, our analytical results 1 and 2 do not dependent on any further assumptions. Although the three simplifying assumptions were made in order to see result 3 more clearly, we did not use assumption 3 in the simulations of Fig. 4.

The analysis presented in this paper also points to the following sobering conclusion: For multiunit correlation analysis to play a useful role in establishing the basic circuitry of the nervous system, new technologies have to be developed for *stable, multiunit* recordings. These requirements stem from the need for extended simultaneous recordings from many cells to construct adequate scatter histograms and to minimize inherent uncertainty due to unobserved but related activities. Unfortunately, neither of these requirements are easily met at present, although extensive efforts towards this goal are underway through the use of silicon-based microelectrode arrays (12).

APPENDIX

Proof of lemma 1. The threshold of neuron B, which is a continuous random variable, has the probability density function and the distribution function denoted $f_{\theta_t^B}(x)$ and $F_{\theta_t^B}(x)$, respectively. Let $b_t = \int_{t_0}^{t} V_\tau^B \, d\tau$, where t_0 is the occurrence instant of the previous spike. From definition of $P_B(t)$ we have

$$P_B(t) = E_{b_t}[f_B(t, \theta_t^B)], \tag{62}$$

where the expectation $E_{b_t}[\cdot]$ is taken with respect to θ_t^B. And

$$\begin{aligned} f_B(t, \theta_t^B) &= \lim_{\Delta t \to 0} \frac{P_r(b_{t+\Delta t} \geq \theta_t^B | b_t < \theta_t^B; \mathcal{H}_t^B, \mathcal{N}_t^B)}{\Delta t} \\ &= \lim_{\Delta t \to 0} \frac{P_r(b_t < \theta_t^B \leq b_{t+\Delta t} | \mathcal{H}_t^B, \mathcal{N}_t^B)}{\Delta t \, P_r(b_t < \theta_t^B | \mathcal{H}_t^B, \mathcal{N}_t^B)} \\ &= V_t^B \frac{f_{\theta_t^B}(b_t)}{1 - F_{\theta_t^B}(b_t)}. \end{aligned} \tag{63}$$

Furthermore, if the threshold is exponentially distributed with mean λ, then $f_{\theta_t^B}(b_t)/[1 - F_{\theta_t^B}(b_t)] = \lambda$, and hence $P_B(t) = \lambda V_t^B$. In this case, $P_B(t)$ does not depend on $\{\mathcal{N}_B(t)\}$, and $\{N_B(t)\}_{t \geq 0}$ evolves without aftereffects.

Proof of lemma 2. Because $\Delta N_B(t)$ can take values 0 and 1 only, by Eq. 3 we have

$$\begin{aligned} &E[V_t^A \frac{\Delta N_B(s)}{\Delta s} | \mathcal{H}_{t \vee s}^B, \mathcal{N}_s^B] \\ &\quad = E\left[\alpha \exp\left\{\sum_{k=1}^{N_B(t)} h(t, T_k^B)\right\} \middle| \Delta N_B(s) = 1; \mathcal{H}_{t \vee s}^B, \mathcal{N}_s^B\right] \\ &\qquad \cdot \frac{P_r(\Delta N_B(s) = 1 | \mathcal{H}_s^B, \mathcal{N}_s^B)}{\Delta s}. \end{aligned} \tag{64}$$

For $t > s$, the conditional expectation in the above equation can be written as

$$\begin{aligned} &E\left[\alpha \exp\left\{\sum_{k=1}^{N_B(t)} h(t, T_k^B)\right\} \middle| \Delta N_B(s) = 1; \mathcal{H}_t^B, \mathcal{N}_s^B\right] \\ &\quad = E\left[\alpha \exp\left\{\sum_{k=1}^{N_B(s)} h(t, T_k^B)\right\} \exp\{h(t, s + \Delta s)\} \right. \\ &\qquad \left. \cdot \exp\left\{\sum_{k=N_B(s+\Delta s)+1}^{N_B(t)} h(t, T_k^B)\right\} \middle| \mathcal{H}_t^B, \mathcal{N}_s^B\right], \end{aligned} \tag{65}$$

which becomes

$$e^{h(t,s)} E[V_t^A | \mathcal{H}_t^B, \mathcal{N}_s^B], \tag{66}$$

as Δs goes to 0. Because $P_B(s)$ is a measurable function with respect to $\sigma(\mathcal{H}_s^B \times \mathcal{N}_s^B)$, we obtain

$$\begin{aligned} E\left[V_t^A \frac{dN_B(s)}{ds}\right] &= e^{h(t,s)} E[E[V_t^A | \mathcal{H}_t^B, \mathcal{N}_s^B] P_B(s)] \\ &= e^{h(t,s)} E[V_t^A P_B(s)]. \end{aligned} \tag{67}$$

For $t \leq s$, we have

$$\begin{aligned} E\left[V_t^A \frac{\Delta N_B(s)}{\Delta s} | \mathcal{H}_s^B, \mathcal{N}_s^B\right] &= E[V_t^A | \mathcal{H}_s^B, \mathcal{N}_s^B] E\left[\frac{\Delta N_B(s)}{\Delta s} | \mathcal{H}_s^B, \mathcal{N}_s^B\right] \\ &= E[V_t^A | \mathcal{H}_s^B, \mathcal{N}_s^B] \frac{P_r(\Delta N_B(s) = 1 | \mathcal{H}_s^B, \mathcal{N}_s^B)}{\Delta s}, \end{aligned} \tag{68}$$

hence

$$E\left[V_t^A \frac{dN_B(s)}{ds}\right] = E[E(V_t^A|\mathcal{H}_s^B, \mathcal{N}_s^B) P_B(s)] = E[V_t^A P_B(s)]. \quad (69)$$

Because $h(t, s)$ represents a synaptic connectivity, which is a causal system with nonzero transmission delay, $h(t, s) = 0$ for $t \leq s$. Thus lemma 2 holds for all t and s.

Proof of theorem 1. Suppose that assumptions 1 and 2 hold, and that the threshold θ_t has an exponential distribution with mean 1. Then

$$\lim_{\Delta t \to 0} \frac{P_r[\Delta N_A(t) = 1|\mathcal{H}_t^A, \mathcal{N}_t^A]}{\Delta t} = V_t^A, \quad (70)$$

hence spike train $N_A(t)$ represents a doubly stochastic Poisson process with the intensity process $\{V_t^A: t \geq 0\}$. Therefore, by Eqs. 31 we have

$$P_A(t) = E(V_t^A|\mathcal{H}_t^B). \quad (71)$$

We choose Δt and Δs such that $s < s + \Delta s < t < t + \Delta t$, or $t < t + \Delta t < s < s + \Delta s$. Because Poisson process is an independent increments process, the conditional probability given the firing histories of neurons A and B can be split into

$$P_r[\Delta N_A(t) = 1, \Delta N_B(s) = 1|\mathcal{H}_t^A, \mathcal{H}_{t\vee s}^B] = P_r[\Delta N_A(t) = 1|\mathcal{H}_t^A]\, P_r[\Delta N_B(s) = 1|\mathcal{H}_t^A, \mathcal{H}_{t\vee s}^B]. \quad (72)$$

By Eq. 31, the first factor is

$$P_r[\Delta N_A(t) = 1|\mathcal{H}_t^A] = V_t^A \Delta t + o(\Delta t). \quad (73)$$

We write the second factor as

$$P_r(\Delta N_B(s) = 1|\mathcal{H}_t^A, \mathcal{H}_{t\vee s}^B) = E[\Delta N_B(s)|\mathcal{H}_t^A, \mathcal{H}_{t\vee s}^B], \quad (74)$$

and we have

$$P_r[\Delta N_A(t) = 1, \Delta N_B(s) = 1|\mathcal{H}_t^A, \mathcal{H}_{t\vee s}^B] = E[V_t^A \Delta N_B(s)|\mathcal{H}_t^A, \mathcal{H}_{t\vee s}^B] + o(\Delta t). \quad (75)$$

By taking average over the σ-field $\mathcal{H}_t^A$, we obtain

$$P_{AB}(t, s) = E\left[V_t^A \frac{dN_B(s)}{ds} \,\middle|\, \mathcal{H}_{t\vee s}^B\right], \quad (76)$$

which is, by the proof of lemma 2,

$$P_{AB}(t, s) = e^{h(t,s)} E[V_t^A|\mathcal{H}_t^B] P_B(s) = e^{h(t,s)} P_A(t) P_B(s). \quad (77)$$

Proof of theorem 2. This can be found in reference 20.

Proof of theorem 3. For a given significance level α, we need to find a bound b satisfying

$$P_r\left(\left|\frac{H_{mn}^{AB}}{H_m^A H_n^B} - 1\right| > b \mid H_m^A, H_n^B; \mathcal{H}_0\right) = \alpha. \quad (78)$$

Let us remember that RH_{mn}^{AB} is binomially distributed with parameters $(R, E[P_{AB}(t, s)])$ and that $H_{mn}^{AB} \to H_m^A H_n^B$ almost surely under $\mathcal{H}_0$. By the central limiting theorem and theorems on limiting distributions,

$$\frac{RH_{mn}^{AB} - RE[H_{mn}^{AB}]}{\sqrt{RH_{mn}^{AB}(1 - H_{mn}^{AB})}} \to N(0, 1) \quad \text{as } R \to \infty, \quad (79)$$

where $N(0, 1)$ is denoted as a standard Gaussian random variable. Then if spike trains A and B are uncorrelated, we approximately write

$$\frac{RH_{mn}^{AB} - RE[H_{mn}^{AB}]}{\sqrt{RH_{mn}^{AB}(1 - H_{mn}^{AB})}} \simeq \frac{RH_{mn}^{AB} - RH_m^A H_n^B}{\sqrt{RH_m^A H_n^B(1 - H_m^A H_n^B)}}. \quad (80)$$

This means that Eq. 78 can be approximately written as

$$P_r(|N(0, 1)| > \epsilon_b \mid \mathcal{H}_0) = \alpha, \quad (81)$$

where

$$\epsilon_b \simeq \frac{bRH_m^A H_n^B}{\sqrt{RH_m^A H_n^B(1 - H_m^A H_n^B)}}, \quad (82)$$

which results in an expression of the bound as

$$b \simeq \epsilon_b \sqrt{\frac{1 - H_m^A H_n^B}{RH_m^A H_n^B}}. \quad (83)$$

The value of ϵ_b is determined by

$$\Phi(\epsilon_b) = 1 - \frac{\alpha}{2}, \quad (84)$$

where

$$\Phi(x) = \frac{1}{\sqrt{2\pi}} \int_{-\infty}^{x} e^{-x^2/2}\, dx.$$

The above arguments imply that element $H_{mn}^{AB}/(H_m^A H_n^B)$ of the normalized joint PST diagram has a conditional expectation value 1 and an approximate conditional variance

$$\sigma_{mn}^2 \simeq \frac{1 - H_m^A H_n^B}{RH_m^A H_n^B} \quad (85)$$

under hypothesis $\mathcal{H}_0$.

Proof of theorem 4. let us note that under hypothesis $\mathcal{H}_0$, $H_{mn}^{AB}/(H_m^A H_n^B)$ is approximately Gaussian distributed with mean 1 and variance σ_{mn}^2. Hence,

$$|G_k - 1| \simeq \left|\frac{1}{N - |k|} \sum_{n=\max(1,1-k)}^{\min(N,N-k)} \sigma_{n+k,n} N_n(0, 1)\right|, \quad (86)$$

where each $N_n(0, 1)$ approximately has a standard Gaussian distribution expressed by

$$N_n(0, 1) = \frac{RH_{n+k,n}^{AB} - RH_{n+k}^A H_n^B}{\sqrt{RH_{n+k}^A H_n^B(1 - H_{n+k}^A H_n^B)}}, \quad (87)$$

and σ_{mn}^2 is given in Eq. 55. Therefore, $G_k - 1$ is approximately Gaussian distributed with zero-mean and variance

$$Var(G_k - 1) = \frac{1}{(N - |k|)^2} \sum_{n=\max(1,1-k)}^{\min(N,N-k)} \sigma_{n+k,n}^2, \quad (88)$$

where mutual independence of $N_n(0, 1)$ is assumed. Let

$$\epsilon_b = \frac{b_k}{\sqrt{Var(G_k - 1)}}, \quad (89)$$

we obtain

$$P_r(|G_k - 1| > b_k \mid H_m^A, H_n^B; \mathcal{H}_0) = 2[1 - \Phi(\epsilon_b)]. \quad (90)$$

If all σ_{mn}^2's are the same, observing the bound b in theorem 3 completes the proof.

The authors would like to express their appreciation to Dr. James Fleshman and to the referees for the valuable comments and suggestions.

This work was supported in part by grants from the Whitaker Foundation and the Naval Research Laboratory.

Received for publication 26 May 1989 and in Final Form 12 October 1989.

REFERENCES

1. Abeles, M. 1982. Local Cortical Circuits: An Electrophysiological Study. Springer-Verlag, Berlin.
2. Ables, M., and M. H. Goldstein. 1977. Multispike train analysis. *Proc. IEEEE (Inst. Electr. Electron. Eng.)* 65:762–772.
3. Bishop, P. B., W. R. Levick, and W. O. Williams. 1964. Statistical analysis of the dark discharge of lateral geniculate neurones. *J. Physiol. (Lond.)*. 170:598–612.
4. van den Boogaard, H., G. Hesselmans, and P. Johannesma. 1986. System identification based on point processes and correlation densities. I. The nonrefractory neuron model. *Math. Biosci.* 80:143–171.
5. van den Boogaard, H. 1988. System identification based on point processes and correlation densities. II. The refractory neuron model. *Math. Biosci.* 91:35–65.
6. Brillinger, D. R. 1975. The identification of point process systems. *Ann. Probability*. 3:909–924.
7. Correia, M. J., and J. P. Landolt. 1977. A point process analysis of the spontaneous activity of anterior semicircular canal units in the anesthetized pigeon. *Biol. Cybern.* 27:199–213.
8. Gerstein, G. L. 1970. Functional association of neurons: Detection and interpretation. *In* The Neurosciences Second Study Program. F. O. Scmitt, editor. Rockefeller University Press, New York. 648–661.
9. Gerstein, G. L., and D. H. Perkel. 1969. Simultaneously recorded trains of action potentials: analysis and functional interpretation. *Science (Wash. DC)*. 148:828–830.
10. Habib, M. K., and P. K. Sen. 1985. Non-stationary stochastic point-process models in neurophysiology with applications to learning. *In* Biostatistics: Statistics in Biomedical, Public Health and Environmental Sciences. P. K. Sen, editor. Elsevier/North-Holland, Amsterdam. 481–509.
11. Knox, C. K. 1974. Cross-correlation functions for a neuronal model. *Biophys. J.* 14:567–582.
12. Krüger, J. 1983. Simultaneous individual recordings from many cerebral neurons: techniques and results. *Rev. Physiol. Biochem. Exp. Pharmacol.* 98:177–233.
13. Nakahama, H., H. Suzuki, H. Yamamoto, S. Aikawa, and S. Nishioka. 1968. A statistical analysis of spontaneous activity of central single neurons. *Physiol. & Behav.* 3:745–752.
14. Palm, G., A. M. H. J. Aertsen, and G. L. Gerstein. 1988. On the significance of correlations among neuronal spike trains. *Biol. Cybern.* 59:1–11.
15. Perkel, D. H., G. L. Gerstein, and G. P. Moore. 1967. Neuronal spike trains and stochastic point processes. I. The single spike train. *Biophys. J.* 7:391–418.
16. Perkel, D. H., G. L. Gerstein, and G. P. Moore. 1967. Neuronal spike trains and stochastic point processes. II. Simultaneous spike train. *Biophys. J.* 7:419–440.
17. Snyder, D. L. 1975. Random Point Process. John Wiley & Sons, New York.
18. van Stokkum, I. H. M., P. I. M. Johannesma, and J. J. Eggermont. 1986. Representation of time-dependent correlation and recurrence time functions. *Biol. Cybern.* 55:17–24.
19. Yang, X., and S. A. Shamma. 1988. A totally automated system for the detection and classification of neural spikes. *IEEE (Inst. Electr. Electron. Eng.) Trans. Biomed. Eng.* 35:806–816.
20. Yang, X. 1989. Detection and classification of neural signals and identification of neural networks. Ph.D. Thesis. Electrical Engineering Department, University of Maryland, College Park. In press.